J. Manuf. Innov.
DOI: 10.22055/jomi.2024.39850.1005 Jomi.scu.ac.ir

Journal of Manufacturing Innovations

Research Paper

Finite Element Simulation of Temperature Field and Residual Stress Induced by Surface Welding Process of Mild Steel

Zahra Shahryari[1], Mohammad Laribaghal[1*], Khalil Gheisari[1]

[1]Materials Science and Engineering Department, Faculty of Engineering, Shahid Chamran University of Ahvaz, Ahvaz, Iran

Received: 2022-01-24; Revised: 2022-07-27; 2023-01-15

* Corresponding author: Mohammad Laribaghal (m.lari@scu.ac.ir)

Abstract

The subject of this study is to investigate the effects of surface welding on welding residual stress, analyzing temperature fields, and distortion in low carbon steel. This work aims to simulate residual stresses that appeared during the surface welding of the carbon steel plates via finite element analysis using the ABAQUS software. This analysis includes a finite element model for the thermal and mechanical welding simulation. It also includes a material deposit, temperature-dependent material properties, metal plasticity, and elasticity. The welding simulation was considered as a coupled temperature-displacement analysis. The element birth and death technique was employed for the simulation of filler metal deposition. The residual stress distribution, distortion magnitude, and temperature changes in the center weld metal were obtained. The results showed that applying boundary conditions of mechanical led to a decrease in the plastic strain. In addition, the residual stresses and the temperature fields are

dependent on several factors, which include the different boundary conditions and the pre-heating temperature.

Keywords: Surface welding, Residual stresses, Stress analysis, Finite element method, ABAQUS software

1. Introduction

Welding is a common method for joining metals and alloys. It is used to achieve a specific form from more fundamental geometries in which materials, like sheets and tubes, are provided. Nonetheless, welding is a thermal process causing undesired residual stresses and deformations in welded structures, especially in the case of thin plates, as a result of a combination of thermal expansion, plastic flow, and phase transformation. These stresses often occur around the fusion zone as well as the heat-affected zone (HAZ) [1], [2]. Consequently, without the application of external stresses, residual stresses remain inside the material. These stresses are heavily influenced by structural characteristics such as plate thickness, width, joint type and geometry, material parameters, mechanical and physical qualities at various temperatures. The type of used filler metal as well as the type of welding technique, welding procedure such as current, voltage, arc development speed, feed rate, nozzle to plate distance, and arc efficiency, are all other controlling factors [2]–[4].

The multi-pass welding techniques are commonly used for joining steel structures or other metal alloys, regeneration of machine and equipment parts, as well as for the application of welding coatings (surfacing, hardfacing). Surfacing is a welding process used to apply a hard, wear-resistant layer of metal to surfaces or edges of worn-out parts. It is one of the most economical methods of conserving and extending the life of machines, tools, and construction equipment. Surfacing, sometimes known as hardfacing or wearfacing, is often used to build up worn shafts, gears, or cutting edges [5], [6].

Residual compressive stresses on the structural components depending on their size can be useful or harmful. Compressive stresses, which have been widely employed to increase component fatigue strength and prevent stress corrosion cracking and brittle fracture, have the optimum impact. Nevertheless, when these stresses become tensile, they weaken the mechanical properties of the welded joints and can lead to catastrophic failure. The presence of tensile residual stresses at or near the boundary between the fusion zone and the HAZ is regarded as the most severe occurrence of residual stresses in the welded joints. To avoid the

negative effects of tensile residual stresses on welding sections, the amount and distribution of tensions must be evaluated, and their value must be reduced or converted to compressive stresses. [2], [4], [7]. As a result, accurate assessment of residual stresses due to welding aids in the development of sound design and structural safety. The precise calculation of residual stresses during welding is difficult because it includes several temperature-dependent material variables [8], [9].

Stress relaxation techniques, diffraction techniques, cracking techniques, and methods based on stress-sensitive characteristics have all been used to measure residual stresses in metals. These strategies do not achieve total stress distribution, and most of them are costly and time-consuming, with some of them being harmful [10], [11]. A trustworthy heat model to describe and analyze the process of heat transfer in the welding technique is required to accurately estimate the welding residual stress field. Engineers, primarily in the aerospace industry, began to apply the finite element technique more regularly in the early 1950s. The use of finite element techniques to study the welding residual stress problem was first employed in 1971 [3], [12]. Recently, researchers have used noticeably numerical methods for predicting the amount of residual stress.

Deng [13] investigated the impact of solid-state phase change on residual stresses and distortions in steels during welding. His findings demonstrated that martensitic transformation had a significant impact on the residual stress and deformation in low and medium carbon steel. With a finite element elastic-plastic thermal stress package, Free et al. [14] calculated the residual stresses of three-dimensional welding and deformations by the thickness of a multi-pass weld in the as-fabricated condition. The thermomechanical behavior and residual stresses were studied using finite element techniques by Akbari et al. [2], who found that the welding heat input has a substantial impact on the residual stresses. Deng et al. [15] compared the distribution of residual stresses in pipelines SUS304 by using a finite element method and experimental method. Punitharani et al. [1] predicted the residual stresses in a hard-faced gate valve with the help of finite element analysis. Gurney [16] has calculated the residual stresses resulting from spot heating at the center of a large circular plate through a form of finite-element analysis and the use of a theoretical, radially symmetrical, temperature distribution. The investigation was concerned in particular with defining the effect of variations in material yield stress, rate of heat input, and peak temperature on the residual-stress distribution. In this paper, the residual stresses and distortions resulting from the process of surface welding on carbon steel are analyzed by the commercial software ABAQUS.

2. Materials and Methods

In this study, distortion, residual stresses, and temperature changes in the welded sample were investigated using a three-dimensional finite element model. The simulation of the process of surface welding has been performed on steel plates. The FE model is shown in Fig.1 with 200 brick elements and 363 nodes and the length, width and thickness are 5 cm, 5 cm, and 0.005 cm, respectively. For the simulated deposit, the molten droplets on the substrate used 100 elements at the length and width of the upper surface plate. Mild steel is used as base metal and stainless steel is used as the deposited material. The temperature-dependent thermal material properties for the plates and the filler weld material can be seen in **Table 1**. The welding parameters, including welding speed and heat input are determined as 2 mm/s and 0.9 kJ/mm, respectively. The different boundary conditions used in this study are shown in **Table 2** and **Fig. 1.**

Furthermore, to consider the effect of preheating temperatures, the given plate was preheated to 300 ℃. Preheating procedure is carried out regarding condition A shown in **Table 2.** Welding direction is also exhibited in **Fig. 2.**

Table 1 Physical and mechanical properties of the used materials

sample	Temperature (℃)	Conductivity (W/m℃)	Density ($Kg.m^{-3}$)	Young's modulus (GPa)	Passions ratio	Specific heat (J/Kg℃)
Base metal	0	43.5	7810	210	0.3	473.8
	200	42.5	7810	210	0.3	502
	400	37.7	7810	210	0.3	551.9
Weld metal	0	14.6	8037	198.5	0.294	462
	200	16.1	8037	198.5	0.294	512
	400	18	8037	198.5	0.294	540

Table 2 Different boundary conditions in this model

Conditions / plate	U1	U2	U3	UR1	UR2	UR3
A	0	0	0	Change in nodes	Chang in nodes	Chang in nodes
B	Chang in nodes	Chang in nodes	Chang in nodes	Chang in nodes	Chang in nodes	Chang in nodes
C	0	0	0	0	0	0

U1: displacement in the y direction

U2: displacement in the x direction

U3: displacement in the z direction

UR1: displacement and rotation in y direction

UR2: displacement and rotation in x direction

UR3: displacement and rotation in z direction

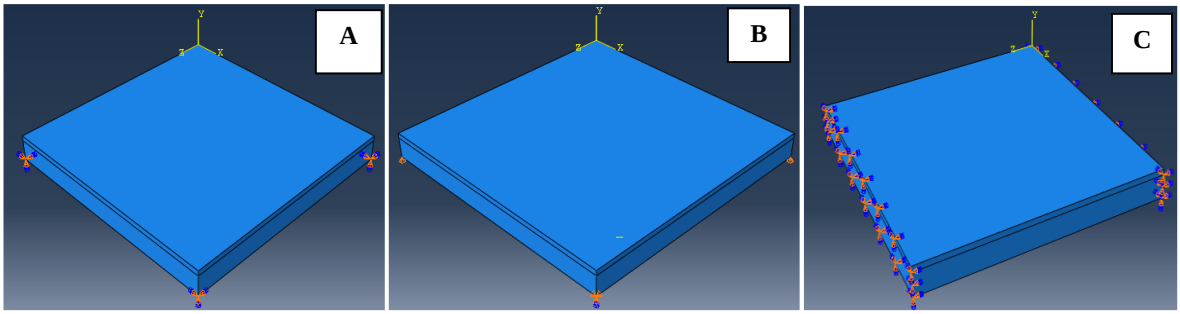

Fig. 1 Mechanical boundary conditions in different states. A: The piece has translational movement in the x, y, and z direction; but no rotational movement in any direction. B: The piece has rotational and translational movement in the x, y, and z direction. C: The piece does not have not rotational and translational movement in the x, y, and z direction

The solution procedure consists of steps from type the coupled temperature displacement – transient and the finite element model employs the technique of element birth and death. At first, all the elements had to be deactivated in one step, and subsequently, the elements were reactivated one by one in each step by form of the model change technique. The initial temperature sample was defined as 25 ℃. Sensitivity analysis for mesh density has been performed and the most appropriate mesh has been selected. The mesh intended in the whole process was considered similarly. **Fig. 3.** shows the final meshed model

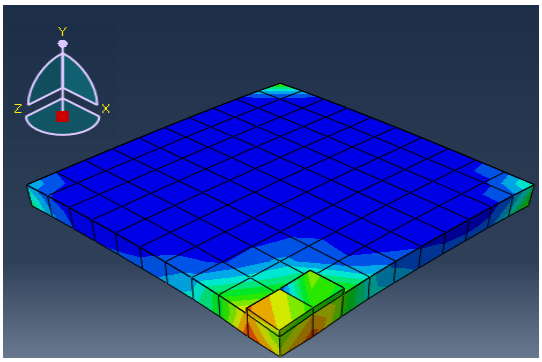

Fig. 2: Welding direction during welding.

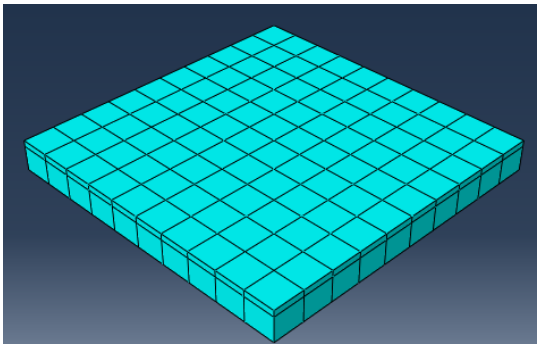

Fig. 3 Meshed Model of Finite Element

3. Results and Discussion

3.1 Thermal analysis

After inserting appropriate boundary conditions into the model, the thermal analysis was carried out. The boundary condition must be applied under the experimental approach. Thermal Analysis is a 3D-thermal heat transfer. In this analysis, the equation for transient heat transfer is shown by Eq. 1 [17]:

$$\rho c \frac{\partial T}{\partial t}(x.y.z.t) = -\nabla \cdot \vec{q}(x.y.z.t) + Q\,(x.y.z.t) \qquad \text{(Eq. 1)}$$

where ρ is the density of the material, C is the specific heat capacity, T is the temperature, q is the heat flux, Q is the internal heat, t is the time, x, y and z are the coordinates in the reference system, and ∇ is the spatial gradient operator. Han et al. [18] numerically examined the temperature field induced by laser beam welding (LBW) in a thin-plate stainless steel AISI304 joint. Their findings showed that the temperature gradients in the fusion zone and its surroundings are quite significant. In this study, for the whole condition, the piece heat input was modeled as distributed heat flux that focused on the welding lines. This heat is spread around by conduction. **Fig. 4** shows the temperature variations in the different welding conditions (**Table 2**) for the preheated condition. It shows that the change in boundary conditions of mechanics cause different temperature changes. The temperature variations in step 11 in the initial weld line deposited on base metal were considered. According to these figures, it can be seen that temperature increases to 900 ℃ in near the weld line but decreases to 100 ℃ when getting away from it. The change of temperature is greater in near points than farther points.

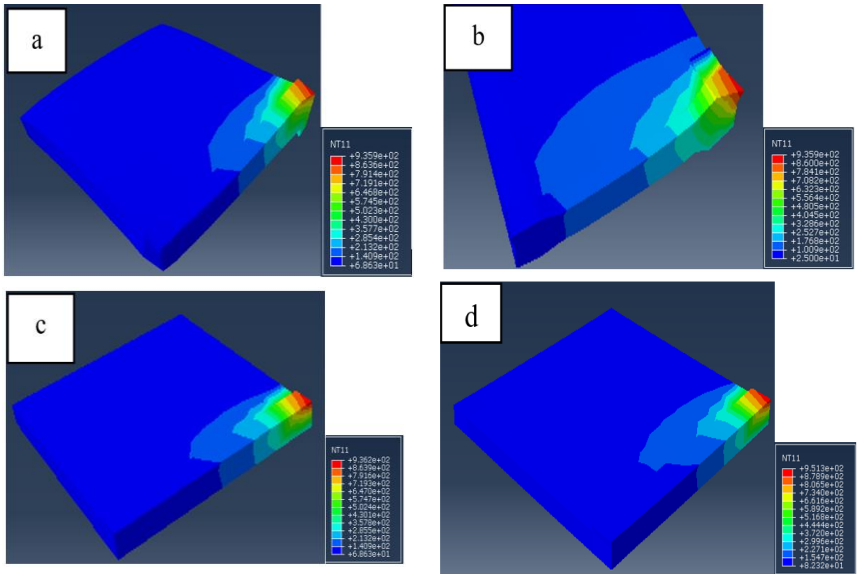

Fig. 4 Thermal cycles for the conditions a) A, b) C, c) B, and d) of the preheated state shown in **Table 2**

According to **Fig. 4**, temperature changes in all conditions are the same, although the value of the temperature distribution in conditions b and d is higher than in other states. This is due to boundary conditions, temperature conditions, and base metal preheating. When molten droplets splatter on a metal surface, they cause the upper temperature for the base metal in step11. This subject causes minimal displacement in this base metal compared with other cases presented in the literature review. According to Sumana and his coworkers [19], preheating minimizes the temperature gradient across the weld in the transverse direction and has a good influence on residual deformations and stresses.

3.2 distortion and residual stresses

To study welding conditions for the given piece, the state in which the bottom of four corners in base metal has the degree of freedom 0 in transitional and rotational modes around the axis coordinate system is considered (condition A in **Table 2** and **Fig. 1**). The results revealed that at the initial modes with a temperature 25 ℃, the collision of molten droplets on the base metal surface leads to change of displacement around the U2 axis at the center of the piece and in line with X-axis, as shown in **Figs. 5 & 6.** These displacement changes were in such a way that they had a decreasing trend in their direction of progress and then gradually went speed up and remained constant at the endpoint of their direction. While in the base piece exposed to preheating conditions at a temperature of 300 ℃, an intense decrease has been observed followed by a sharp increase and finally remains constant.

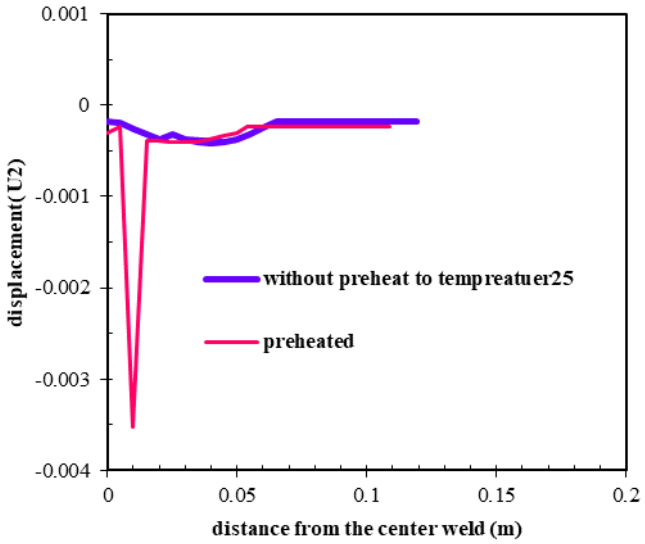

Fig. 5 Displacement in the direction U2 in preheated and without preheating states

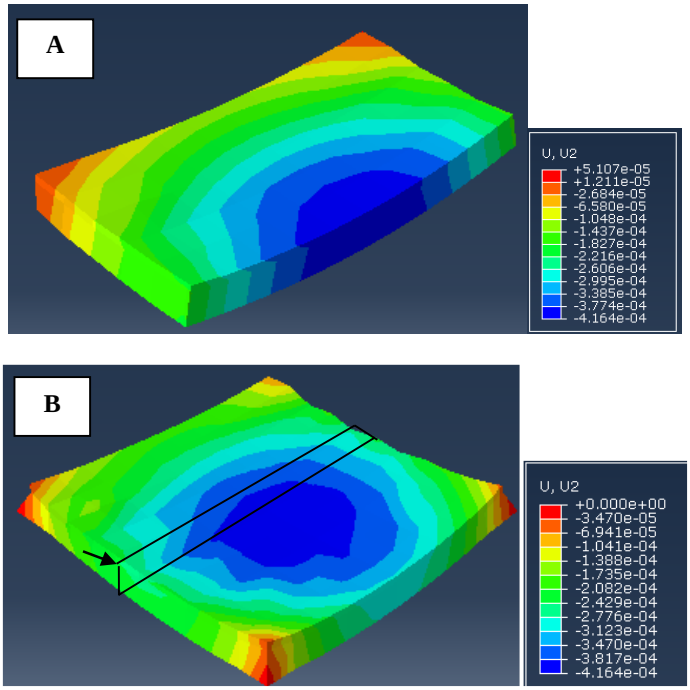

Fig. 6 Change of displacement in the direction U2 in the un-preheated (A) and preheated (B) states

The non-uniform expansion and contraction of the weld and surrounding base material generated by the heating and cooling cycle during the welding process cause distortion in a welded structure. The distortion in a welded structure can be reduced by designing suitable junction placements and/or altering plate thickness during the design stage. Meanwhile, during the production stage, controlling heat input and using the suitable assembly sequence might help to limit welding-induced deformation to some extent [20], [21]. According to the graphs, preheating of base metal leads to a decrease in displacement range at the given direction. This is in line with the expected state. Preheating of the base metal, the input temperature comes down and droplet temperatures go up, so displacement is low. Nevertheless, the highest amount of strain in the case of non-preheating is less than the case of preheating at 300 °C. The reason for this can be the collision of molten droplets with base metal leads to a lot of displacement because of the being cool of piece in an initial state. **Figs. 7 & 8** show the changes in plastic strain in the substrate in the preheated and un-preheated states.

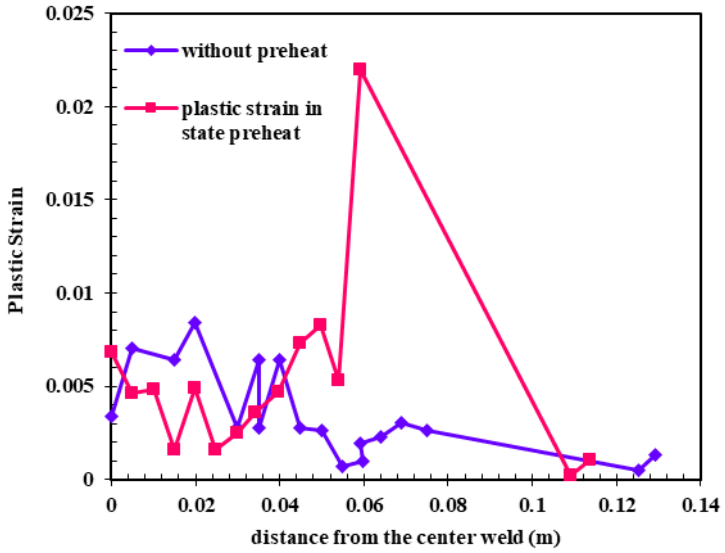

Fig. 7 The variations in the plastic strain in the preheated and un-preheated states

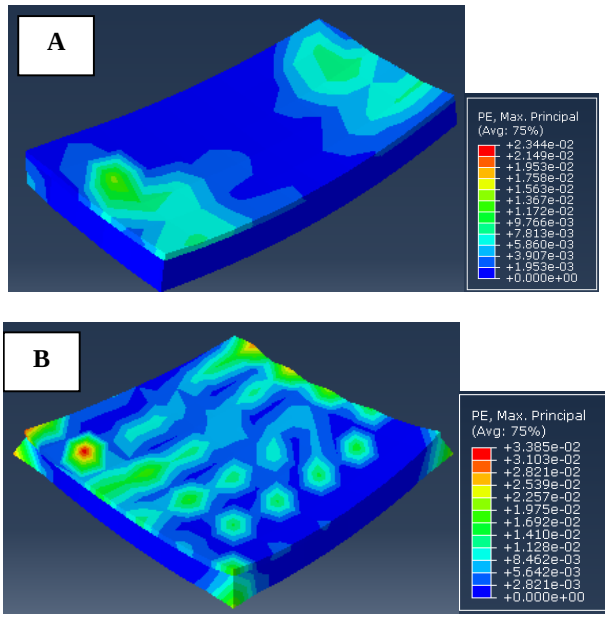

Fig. 8 Plastic strain in the un-preheated (A) and preheated (B) states

Figs 9 & 10 exhibit the effect of preheating temperature on residual stress after surface welding of base metal. As shown, when the base metal has a temperature of 25 °C, the residual stress increases gradually based on direction displacement and then progressing from the front piece to the rear. But in the case of preheating, the residual stress increases at the beginning of the displacement direction, and then it decreases. This behavior can be attributed to the heating of the piece till the endpoint and finally reducing stress. According to the Lee et al. findings [6], preheating can significantly lower final tensile residual stress, particularly around the weld toe

and at the bottom of the chord plate. Based on their findings, the transverse residual stresses at the weld toe for joints with and without preheating are 316.5 MPa and 408.7 MPa, respectively [14]. Charkhi and his coworker [22] observed that preheating of the carbon steel pipes reduces tensile hoop residual stresses on the inner surface as well as tensile axial stresses on both the inner and outer surfaces.

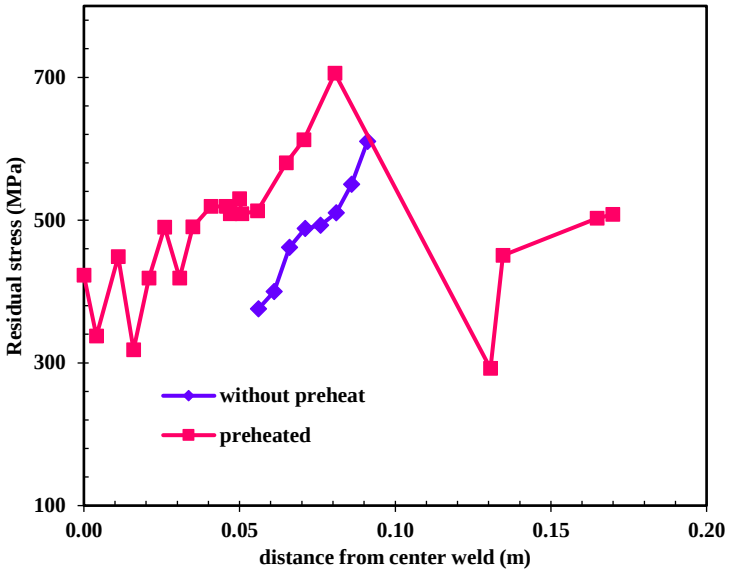

Fig 9 The residual stress variations on the plate in the preheated and un-preheated conditions

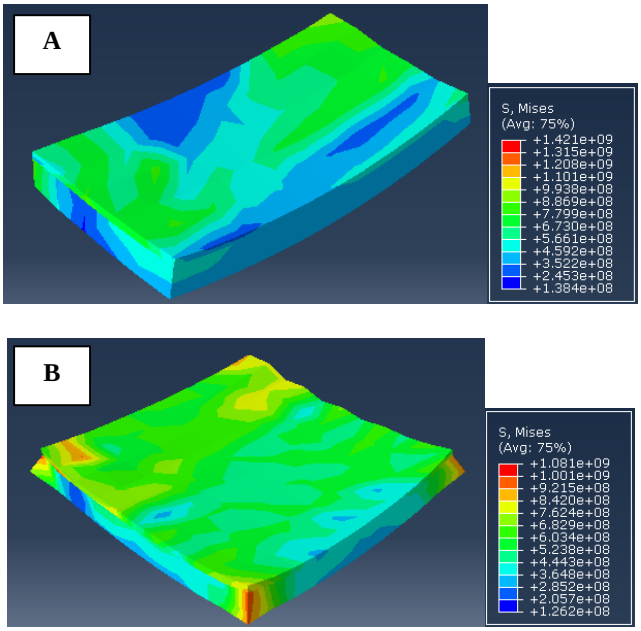

Fig 10 Residual stress variations on the plate in the un-preheated (A) and preheated (B) conditions

To change the base metal conditions, the other situations are also considered in which the piece has different boundary conditions. Two different boundary conditions corresponding to the fixed, pinned and simple supports were considered. The change in this trend in creating boundary conditions leads to changes in residual stress, displacement, and strain compared to the previous state.

As it was expected, because of the conditions limiting the rotation, residual stress reached higher amounts of previous states in preheating and non-preheating at the beginning of direction as shown in **Fig. 11**. Then it comes down and becomes similar to a preheating state. Changes in displacement and strain mode are shown in **Fig. 12**.

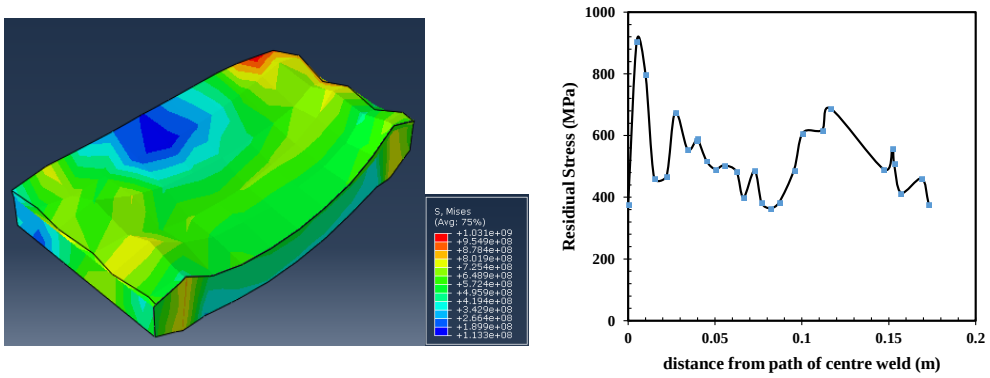

Fig. 11 Residual stress changes in condition C, in **Table 2**

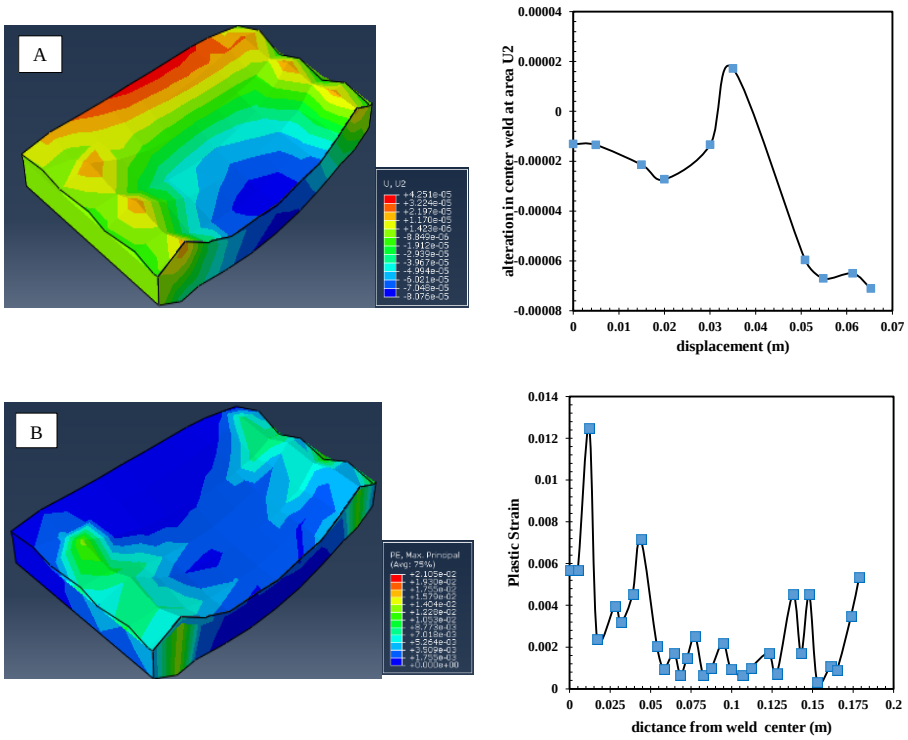

Fig, 12 The variations of displacement in the direction U2 (A) and plastic strain (B) in the plate in condition C, in **Table 2**

Other different boundary conditions are imposed on base metal as shown in **Fig. 13**. According to this figure, the residual stress will be increased by moving away from the direction. This behavior can be ascribed to imposed constraints and the rotation ability of the piece in some directions. By entering droplets on base metal and creating a coat on its surface, the amount of residual stress is approximately similar to the state in which the piece is created under all imposed constraints at the four corners of the piece.

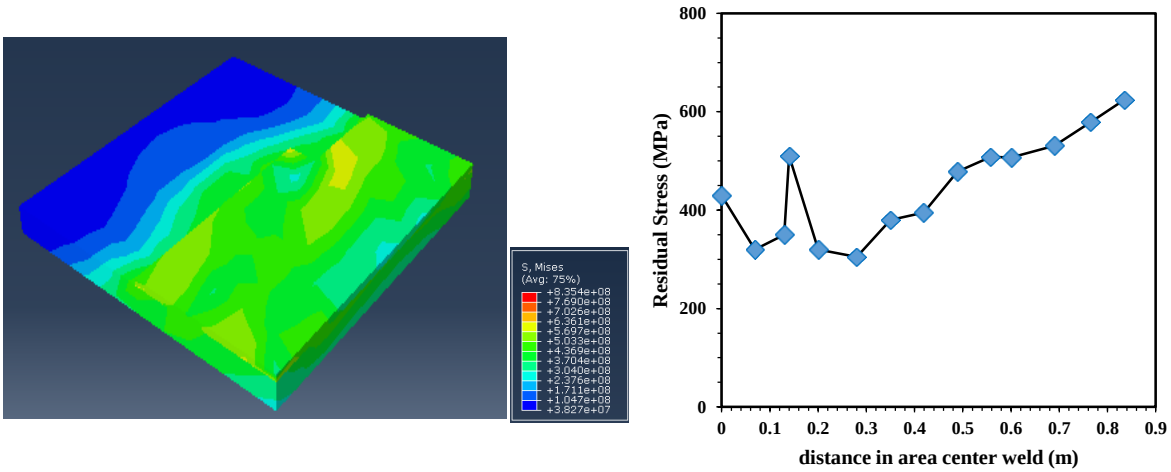

Fig. 13 Residual stress variations in condition B, in **Table 2**

These findings show that the computation finite element results are very close to the boundary condition and initial condition of this piece.

4. Conclusions

In the present study, a comprehensive finite element model was developed for predicting and calculating the residual stresses, distortion, and changes in temperature in the center of weld metal caused by the manual metal arc surface welding of carbon steel plates. The most important findings of this study can be summarized as follows:

- Preheating of base metal leads to a decrease in displacement range in a given direction.
- Preheating of the base metal decreases the value of the residual stress in comparison with the un-preheated state.
- The changing in mechanical boundary conditions leads to changes in temperature of different welding steps.

References

[1] K. Punitharani, N. Murugan, and S. Sivagami, “Finite element analysis of residual stresses and distortion in hard faced gate valve,” *J. Sci. Ind. Res. (India).*, vol. 69, Feb. 2010.

[2] D. Akbari and I. Sattari-Far, “Effect of the welding heat input on residual stresses in butt-welds of dissimilar pipe joints,” *Int. J. Press. Vessel. Pip.*, vol. 86, no. 11, pp. 769–776, Nov. 2009, doi: 10.1016/j.ijpvp.2009.07.005.

[3] Y. S. Yegaie, A. Kermanpur, and M. Shamanian, “Numerical simulation and experimental investigation of temperature and residual stresses in GTAW with a heat sink process of Monel 400 plates,” *J. Mater. Process. Technol.*, vol. 210, no. 13, pp. 1690–1701, Oct. 2010, doi: 10.1016/j.jmatprotec.2010.05.017.

[4] A. Yaghi, T. H. Hyde, A. A. Becker, W. Sun, and J. A. Williams, “Residual stress simulation in thin and thick-walled stainless steel pipe welds including pipe diameter effects,” *Int. J. Press. Vessel. Pip.*, vol. 83, no. 11–12, pp. 864–874, Nov. 2006, doi: 10.1016/j.ijpvp.2006.08.014.

[5] R. Koňár, M. Mičian, M. Málek, J. Šutka, M. Gucwa, and J. Winczek, “Numerical simulation of a temperature field during multi-beads surface welding,” *J. Appl. Math. Comput. Mech.*, vol. 20, no. 1, pp. 49–59, Mar. 2021, doi: 10.17512/jamcm.2021.1.05.

[6] M. H. Sar, O. S. Barrak, and S. K. Hussain, “Effect of Multi-pass SMAW Welding on the Surface Hardness and Microstructure of Carbon Steel AISI 1050,” *IOP Conf. Ser. Mater. Sci. Eng.*, vol. 1105, no. 1, p. 012058, Jun. 2021, doi: 10.1088/1757-899X/1105/1/012058.

[7] G. S. Brar, “Residual Stresses in Butt Welding of Two Circular Pipes: An Experimental and Numerical Investigation,” in *Volume 1: Codes and Standards*, American Society of Mechanical Engineers, Jul. 2014. doi: 10.1115/PVP2014-29082.

[8] C. K. Lee, S. P. Chiew, and J. Jiang, “Residual stress study of welded high strength steel thin-walled plate-to-plate joints part 2: Numerical modeling,” *Thin-Walled Struct.*, vol. 59, pp. 120–131, Oct. 2012, doi: 10.1016/j.tws.2012.04.001.

[9] D. Venkatkumar and D. Ravindran, “3D finite element simulation of temperature distribution, residual stress and distortion on 304 stainless steel plates using GTA

welding," *J. Mech. Sci. Technol.*, vol. 30, no. 1, pp. 67–76, Jan. 2016, doi: 10.1007/s12206-015-1208-5.

[10] I. Stamenkovic, D. and Vasovic, "Finite Element Analysis of Residual Stress in Butt Welding Two Similar Plates.," 2009.

[11] M. S. Olufsen, C. S. Peskin, W. Y. Kim, E. M. Pedersen, A. Nadim, and J. Larsen, "Numerical Simulation and Experimental Validation of Blood Flow in Arteries with Structured-Tree Outflow Conditions," *Ann. Biomed. Eng.*, vol. 28, no. 11, pp. 1281–1299, Nov. 2000, doi: 10.1114/1.1326031.

[12] T.-L. Teng, C.-P. Fung, P.-H. Chang, and W.-C. Yang, "Analysis of residual stresses and distortions in T-joint fillet welds," *Int. J. Press. Vessel. Pip.*, vol. 78, no. 8, pp. 523–538, Aug. 2001, doi: 10.1016/S0308-0161(01)00074-6.

[13] D. Deng, "FEM prediction of welding residual stress and distortion in carbon steel considering phase transformation effects," *Mater. Des.*, vol. 30, no. 2, pp. 359–366, Feb. 2009, doi: 10.1016/j.matdes.2008.04.052.

[14] J. A. Free and R. F. D. Porter Goff, "Predicting residual stresses in multi-pass weldments with the finite element method," *Comput. Struct.*, vol. 32, no. 2, pp. 365–378, Jan. 1989, doi: 10.1016/0045-7949(89)90048-5.

[15] D. Deng and H. Murakawa, "Numerical simulation of temperature field and residual stress in multi-pass welds in stainless steel pipe and comparison with experimental measurements," *Comput. Mater. Sci.*, vol. 37, no. 3, pp. 269–277, Sep. 2006, doi: 10.1016/j.commatsci.2005.07.007.

[16] T. R. Gurney, "Residual stresses in a large circular disc caused by local heating and cooling at its centre," *J. Strain Anal. Eng. Des.*, vol. 6, pp. 89–98, 1971, [Online]. Available: https://api.semanticscholar.org/CorpusID:135968396

[17] D. Deng and H. Murakawa, "Prediction of welding distortion and residual stress in a thin plate butt-welded joint," *Comput. Mater. Sci.*, vol. 43, no. 2, pp. 353–365, Aug. 2008, doi: 10.1016/j.commatsci.2007.12.006.

[18] H. GuoMing, Z. Jian, and L. JianQang, "Dynamic simulation of the temperature field of stainless steel laser welding," *Mater. Des.*, vol. 28, no. 1, pp. 240–245, Jan. 2007, doi: 10.1016/j.matdes.2005.06.006.

[19] S. Suman and P. Biswas, “Comparative study on SAW welding induced distortion and residual stresses of CSEF steel considering solid state phase transformation and preheating,” *J. Manuf. Process.*, vol. 51, pp. 19–30, Mar. 2020, doi: 10.1016/j.jmapro.2020.01.012.

[20] P. Michaleris, *Minimization of Welding Distortion and Buckling: Modelling and Implementation*. 2011.

[21] J. Sun, X. Liu, Y. Tong, and D. Deng, “A comparative study on welding temperature fields, residual stress distributions and deformations induced by laser beam welding and CO2 gas arc welding,” *Mater. Des.*, vol. 63, pp. 519–530, Nov. 2014.

[22] M. Charkhi and D. Akbari, “Experimental and numerical investigation of the effects of the pre-heating in the modification of residual stresses in the repair welding process,” *Int. J. Press. Vessel. Pip.*, vol. 171, pp. 79–91, Mar. 2019, doi: 10.1016/j.ijpvp.2019.02.006.